THE JOURNAL OF BIOLOGICAL CHEMISTRY VOL. 289, NO. 45, pp. 31029–31042, November 7, 2014

The Essential Protein for Bacterial Flagella Formation FlgJ Functions as a β-*N*-Acetylglucosaminidase*[S]

Received for publication, August 8, 2014, and in revised form, September 10, 2014 Published, JBC Papers in Press, September 23, 2014, DOI 10.1074/jbc.M114.603944

Francesca A. Herlihey, Patrick J. Moynihan[1], and Anthony J. Clarke[2]

From the Department of Molecular and Cellular Biology, University of Guelph, Guelph, Ontario N1G 2W1, Canada

Background: FlgJ is required for flagella formation in *Salmonella enterica*.
Results: The lytic activity of FlgJ was determined to be that of a β-*N*-acetylglucosaminidase using a novel assay.
Conclusion: FlgJ is a hydrolase and not a lytic transglycosylase.
Significance: This information is essential for the search and rational design of inhibitors that may serve as leads to a new class of antibiotics.

The flagellum is a major virulence factor of motile pathogenic bacteria. This structure requires more than 50 proteins for its biogenesis and function, one of which is FlgJ. Homologs of FlgJ produced by the β- and γ-proteobacteria, such as *Salmonella enterica*, *Vibrio* spp., and both *Sphingomonas* sp. and *Pseudomonas* spp. are bifunctional, possessing an N-terminal domain responsible for proper rod assembly and a C-terminal domain possessing peptidoglycan lytic activity. Despite the amount of research conducted on FlgJ from these and other bacteria over the past 15 years, no biochemical analysis had been conducted on any FlgJ and consequently confusion exists as to whether the enzyme is a peptidoglycan hydrolase or a lytic transglycosylase. In this study, we present the development of a novel assay for glycoside lytic enzymes and its use to provide the first enzymatic characterization of the lytic domain of FlgJ from *S. enterica* as the model enzyme. Surprisingly, FlgJ functions as neither a muramidase nor a lytic transglycosylases but rather as a β-*N*-acetylglucosaminidase. As such, FlgJ represents the first autolysin with this activity to be characterized from a Gram-negative bacterium. At its optimal pH of 4.0, the Michaelis-Menten parameters of K_m and k_{cat} for FlgJ from *S. enterica* were determined to be 0.64 ± 0.18 mg ml^{-1} and 0.13 ± 0.016 s^{-1}, respectively, using purified PG as substrate. Its catalytic residues were identified as Glu^{184} and Glu^{223}.

The flagellum is recognized as an important virulence factor of motile pathogenic bacteria allowing them to reach their specific target infection site(s), in addition to avoiding hostile environments, and accessing nutrients (1). The biogenesis of the flagellar system is best understood for members of *Enterobacteriaceae*, in particular *Salmonella enterica*. *Salmonella* serotypes are of interest because adherence of flagella to surfaces contributes to food contamination (*e.g.* 2) and its strong antigenic properties can provoke inflammatory responses during host infections (*e.g.* Ref. 3).

More than 50 genes are associated with flagellar formation and function in *S. enterica* (reviewed in Ref. 4), which involves 20 different proteins. These proteins form a hetero-oligomeric structure comprised of three major substructures: a basal body that spans the cell wall, a connecting hook, and a thin helical filament that extends into the extracellular environment (5). The basal body consists of an inner ring (MS ring) and two outer rings (L and P rings) connected to a central rod that crosses the cytoplasmic membrane, periplasm, and outer membrane. The rod component proteins are synthesized in the cytosol and transported to the periplasm via the flagellum-specific type III export pathway. This specialized export apparatus exists within a central pore in the MS ring (6–8). During flagella formation, the rod needs to penetrate through the peptidoglycan (PG)[3] layer. At approximately 4 nm (9), the diameter of the rod is larger than the estimated pore size of the PG sacculus (10) and thus its insertion requires the localized and controlled lysis of PG strands.

PG is a heteropolymer of alternating glycan strands and peptide chains forming a rigid network that completely surrounds bacterial cells to maintain the integrity of their cytoplasmic membranes. The glycan strands are composed of repeating *N*-acetylglucosamine (GlcNAc) and *N*-acetylmuramic acid (MurNAc) linked residues β-(1→4) and are cross-linked together through amide linkages between the stem peptides attached to the lactyl groups of MurNAc residues. Once formed, the PG sacculus is not a static structure as it requires constant biosynthesis and reinforcement to permit cellular growth and division. This continuous biosynthesis and turnover are maintained by the concerted action of the extra-cytoplasmic PG-synthesizing enzymes (the penicillin-binding proteins) and PG-lytic enzymes, which provide new sites for the insertion of the PG precursors, in addition to facilitating the separation of daughter cells (reviewed in Ref. 11). Different

* This work was supported by Canadian Institutes of Health Research Team Grant TGC114045 (to A. J. C.) and an Ontario Graduate Scholarship (to P. J. M.) from the Province of Ontario.
[S] This article contains supplemental Fig. S1.
[1] Present address: School of Biosciences, University of Birmingham, Edgbaston, Birmingham B15 2TT, United Kingdom.
[2] To whom correspondence should be addressed. Tel.: 519-824-4120; Fax: 519-837-1802; E-mail: a.clarke@exec.uoguelph.ca.

[3] The abbreviations used are: PG, peptidoglycan; MurNAc, *N*-acetylmuramic acid; GlcNAc, *N*-acetylglucosamine; LT, lytic transglycosylase; Mlt, membrane-bound lytic transglycosylase; Slt, soluble lytic transglycosylase; Ni^{2+}-NTA, Ni^{2+}-nitrilotriacetic acid; HPAEC-PAD, high pH anion-exchange chromatography-pulsed amperometric detection; CHES, 2-(cyclohexylamino)ethanesulfonic acid; PDB, Protein Data Bank.

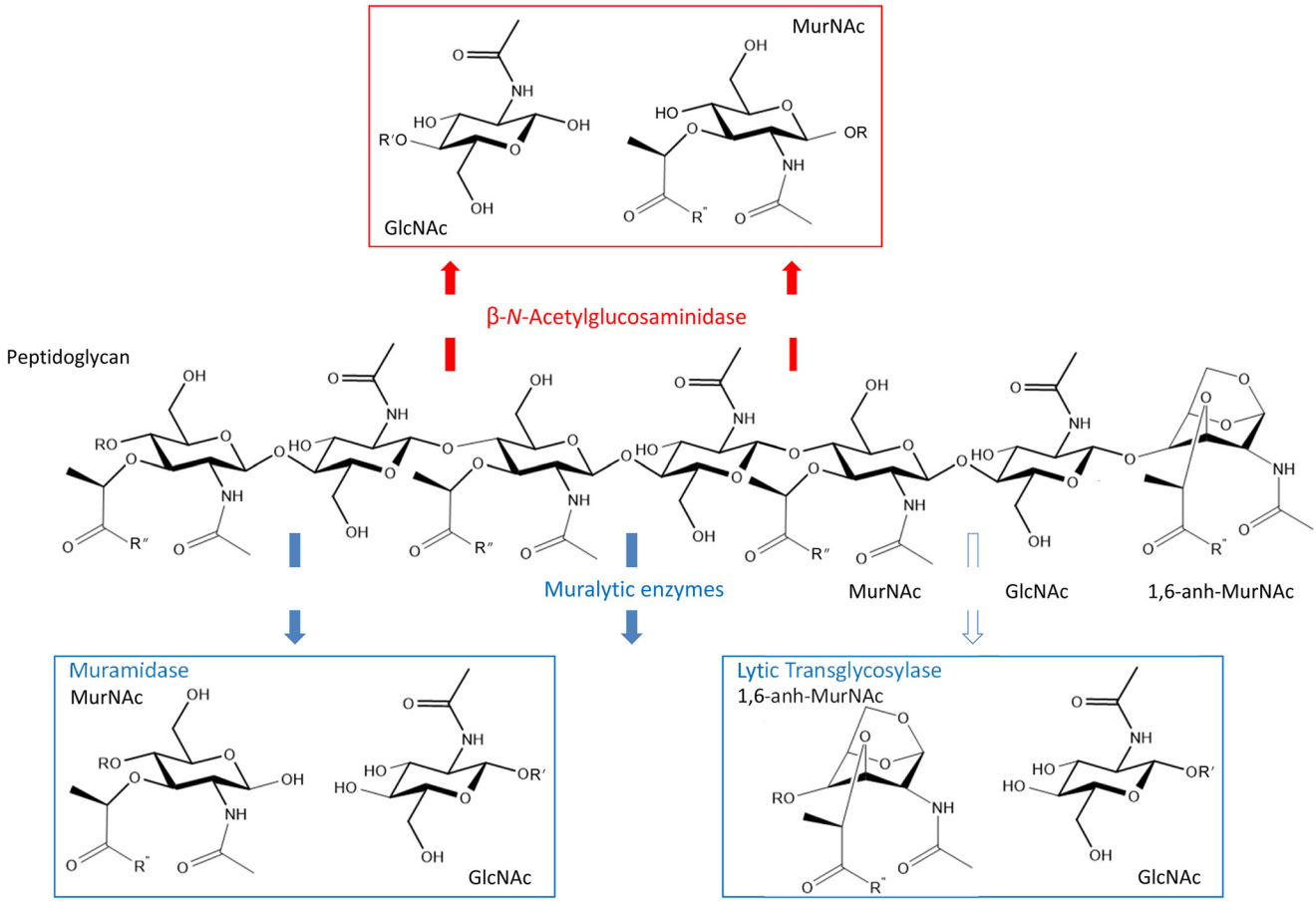

FIGURE 1. **Glycolytic autolysins of bacteria.** The *β-N*-acetylglucosaminidases hydrolyze the *β*-1,4 linkage between GlcNAc and MurNAc residues in PG, whereas the muralytic enzymes, muramidases and LTs, cleave between MurNAc and GlcNAc residues. The muramidases are hydrolytic but the LTs are not; instead they release GlcNAc residues with the concomitant formation of 1,6-anhydroMurNAc. The *open* and *closed arrows* denote exo- and endo-activity, respectively.

classes of lytic enzymes exist for the cleavage of each of the various linkages that exist within PG. Thus, with Gram-negative bacteria, peptidases (both carboxy- and endopeptidases) hydrolyze the peptide bonds linking the amino acids of stem peptides, whereas glycolytic enzymes cleave the *β*-(1→4) linkage between the amino sugars of the carbohydrate chains (recently reviewed in Refs. 12 and 13). Those enzymes that lead to cellular lysis if left uncontrolled are referred to as autolysins.

The predominant site of cleavage within the glycan chains of PG in Gram-negative bacteria is the linkage between MurNAc and GlcNAc residues and this is catalyzed by muralytic enzymes (Fig. 1). Two classes of muralytic enzymes exist, muramidases (EC 3.2.1.17; lysozymes) and lytic transglycosylases (EC 4.2.2.n1/n2; LTs), which differ in the nature of their reaction products. As hydrolases, the muramidases add water across the *β*-(1→4)-glycosidic bond to be cleaved and thereby generate a reducing MurNAc product. Although possessing the structural "lysozyme-fold," the LTs, on the other hand, are not hydrolases. Instead, the LTs catalyze an intramolecular rearrangement involving the C-6 hydroxyl group of the MurNAc at the site of cleavage to effect lysis with the concomitant formation of a 1,6-anhydromuramoyl reaction product (14). The LTs represent a major class of autolysins in Gram-negative bacteria as they play essential roles in the biosynthesis, maintenance, and turnover of the PG sacculus (reviewed in Ref. 15).

The other site of cleavage within the carbohydrate backbone of PG is the *β*-(1→4)-glycosidic linkage between GlcNAc and MurNAc residues and this is catalyzed by *β-N*-acetylglucosaminidases (EC 3.2.1.14; chitinase) (Fig. 1). These enzymes play a more predominant role as autolysins in the metabolism of PG within Gram-positive bacteria (13). However, to date, their autolytic activity has not been detected in any Gram-negative bacterium (11), but a related enzyme, *β-N*-acetylhexosaminidase (EC 3.2.1.52; NagZ), participates in the cytoplasmic events of PG turnover (13).

FlgJ of the flagella operon has been shown to be required for the proper assembly of the flagellum (16). The FlgJs produced by the *β*- and *γ*-proteobacteria, such as *S. enterica*, *Vibrio* spp., and both *Sphingomonas* sp. and *Pseudomonas* spp. are bifunctional, possessing an N-terminal domain responsible for proper rod assembly and a C-terminal domain possessing PG lytic activity (16–21). Despite the amount of research conducted on FlgJ from these and other bacteria, no biochemical analysis has been conducted on any FlgJ and consequently confusion exists as to whether they function as a hydrolase or an LT.

The crystal structure of FlgJ from *Sphingomonas* sp. strain A1, the only one solved, contains a lysozyme-like fold (20, 21) and was classified as a member the glycoside hydrolase family GH73 (20) of the CAZy database thereby reinforcing earlier suggestions that FlgJ is muralytic (16, 19–21, 23). However, the

TABLE 1
Bacterial strains and plasmids used in this study

Strains	Genotype	Source or Ref.
E. coli BL21(λDE3)pLysS	F- *ompT hsdS*B ($r_B^- m_B^-$) *gal dcm rne131* (DE3)pLysS(Cm^r)	Novagen
E. coli DH5α	*fhuA2 lac(del)U169 phoA glnV44 Φ80′ lacZ(del)M15 gyrA96 recA1 relA1 endA1 thi-1 hsdR17*	Invitrogen
S. enterica serovar *typhimurium* LT2	Genome sequence strain	
Plasmids	**Description**	
pET28a(+)	IPTG-inducible T7 expersion vector; N- and C-terminal His_6 tag, K_m^r	Novagen
pACFH4	pET28a (+) derivative containing *flgJ* from LT2 encoding FlgJ truncated by its N-terminal 151 amino acids with an N-terminal His_6 tag on an NdeI/XhoI fragment; K_m^r	This study
pACFH5	pACFH4 derivative encoding FlgJ truncated by its C-terminal 10 amino acids	This study
pACFH6	pACFH5 derivative encoding FlgJ with a $Glu^{184} \rightarrow$ Gln replacement	This study
pACFH8	pACFH5 derivative encoding FlgJ with a $Glu^{223} \rightarrow$ Gln replacement	This study

GH73 family additionally contains *N*-acetylglucosaminidases (EC 3.2.1.14), which also possess the lysozyme-fold (CAZy database). To further complicate the issue, the monofunctional FlgJs of *Rhodobacter sphaeroides* (25) and *Caulobacter crescentus* (26) lack lytic activity and this is compensated for by the production of putative LTs, which for the former bacterium is encoded within its Flg operon. Like other LTs, they too would possess the lysozyme-fold (15).

In this study, we present the development of a novel assay for glycoside lytic enzymes and its use to provide the first enzymatic characterization of the lytic domain of FlgJ from *S. enterica* serovar *typhimurium* (*S. typhimurium*) as the model enzyme. Surprisingly, FlgJ functions as neither a muramidase nor an LT but rather as a β-*N*-acetylglucosaminidase. Thus, it represents the first autolysin with this activity to be characterized from a Gram-negative bacterium.

EXPERIMENTAL PROCEDURES

Chemicals and Reagents

DNase I, RNase A, Pronase, isopropyl β-D-1-thiogalactopyranoside, and EDTA-free protease inhibitor tablets were purchased from Roche Diagnostics (Laval, QC, ON). T4 DNA ligase and restriction enzymes were from New England Biolabs (Mississauga, ON). Ni^{2+}-nitrilotriacetic acid (Ni^{2+}-NTA)-agarose was obtained from Qiagen (Valencia, CA), whereas Source 15S resin was purchased from GE Healthcare. Fischer (Nepean, ON) provided acrylamide, glycerol, and Luria-Bertani (LB) growth medium. Unless otherwise stated, all other chemicals and reagents were from Sigma, and growth media from Difco (Detroit, MI).

Bacterial Strains and Growth

The source of plasmids and bacterial strains used in this study, together with their genotypic description are listed in Table 1. *Escherichia coli* strains DH5α and BL21(λDE3)pLysS were maintained on LB broth or agar at 37 °C, which were supplemented with kanamycin sulfate (50 μg/ml) and chloramphenicol (34 μg/ml) in the case of strains harboring plasmids pET28a(+) and pLysS, respectively. For overexpression studies and protein production, *E. coli* BL21(λDE3)pLysS was grown in SuperBroth (5 g of sodium chloride, 20 g of yeast extract, and 32 g of tryptone) at 30 °C with agitation. All strains were stored at −80 °C in 25% glycerol.

Isolation and Purification of PG

Samples of insoluble PG were isolated from *S. typhimurium* strain LT2 using the boiling SDS protocol and purified by enzyme treatment (amylase, DNase, RNase, and Pronase) as described by Clarke (27).

Conditions for PCR

Chromosomal DNA template for PCR was isolated from *S. typhimurium* LT2. All oligonucleotide primers used in this study are listed in Table 2 and were acquired from Integrated DNA Technologies (Coralville, IA). PCR amplifications were achieved in 50-μl volumes using a Bio-Rad Mycycler Thermal Cycler system. Purification of PCR products was performed using the MinElute PCR Purification kit (Qiagen) or the High Pure PCR Product Purification kit (Roche).

Engineering of flgJ

The *flgJ* ORF was amplified by PCR using the primers that contained NdeI and XhoI sites to facilitate cloning of its 3′-end encoding the C-terminal lytic domain of FlgJ (henceforth termed $FlgJ_C$) and the incorporation of His_6 tag from pET28a(+) at its N terminus. Amplified ORFs were cleaned using a PCR clean up kit, digested with the respective restriction enzymes, and ligated with appropriately digested pET28a(+) plasmid to yield pACFH4, which was then transformed into *E. coli* DH5α. Individual constructs were isolated from transformants, screened for the correct size insert, and sequenced to confirm nucleotide identity (Genomics Facility within the Advanced Analysis Centre, University of Guelph). Initial expression trials demonstrated that the recombinant protein was not stable in its *E. coli* host as it was partially digested. The major fragment was determined to lack its C-terminal 10 amino acids. Hence, a further truncation of *flgJ* was made by removing 30 nucleotides from its 3′ end. PCR products and pET28a(+) were purified and digested with the appropriate restriction enzymes prior to ligation yielding pACFH5. The final protein product, $FlgJ_C$, lacked its 151 N-terminal amino acids and 10 C-terminal amino acids.

Replacement of amino acids for enzymatic activity analysis was achieved using the QuikChange site-directed mutagenesis protocol (Stratagene, La Jolla, CA) with pACFH5 as template. Following PCR amplification of plasmid constructs, products were digested overnight with DpnI and then transformed into

TABLE 2
Oligonucleotide primers used in this study
Nucleotides underlined denote restriction sites and those in bold denote the replacements for site-directed mutagenesis (SDM).

	Primer name	Oligonucleotide sequence (5′-3′)	Target/final vector	Description
1	$FlgJ_{Fwd}$	ATCGCATATGAGTAAAGACTTTCTGGCCCG	pET28a (+)/pACFH4	Forward primer for $FlgJ_C$
2	$FlgJ_{Rev}$	CGATCTCGAGTTAAAAGAGATTGTCGAGATTCG	pET28a (+)/pACFH4	Reverse primer for $FlgJ_C$
3	$FlgJ_{CFwd}$	CGATCTCGAGTTATTTGCTGACCTTTTCAC	pACFH4/pACFH5	Reverse primer for $FlgJ_C$ truncated by 30 nucleotides
4	$FlgJE184Q_{Fwd}$	GATTCTGGCGCAGGCGGCACTG[b]CAGTCCGGCTGGG	pACFH5/pACFH6	Forward primer for SDM of E184Q
5	$FlgJE184Q_{Rev}$	GGCGGCACTG[b]CTGTCCGGCTGGGGGCAGCG	pACFH5/pACFH6	Reverse primer for SDM of E184Q
6	$FlgJE223Q_{Fwd}$	TGACGGAGATCACCACCACT[b]CAATACGAAA	pACFH5/pACFH8	Forward primer for SDM of E223Q
7	$FlgJE223Q_{Rev}$	GCTTCGCCATTTTCGTA[b]TTGAGTGGTGGT	pACFH5/pACFH8	Reverse primer for SDM of E223Q

E. coli DH5α. Selected colonies were sequenced to confirm nucleotide identity and a description of the resulting constructs is presented in Table 1.

Overproduction and Purification of $FlgJ_C$

E. coli BL21(λDE3)pLysS transformed with plasmid DNA was inoculated into SuperBroth supplemented with kanamycin sulfate (50 μg ml^{-1}) and chloramphenicol (34 μg ml^{-1}) and incubated at 37 °C until early exponential phase ($A_{600\,nm} \sim 0.6$). Freshly prepared isopropyl β-D-1-thiogalactopyranoside was added to a final concentration of 1 mM and expression was induced for 4 h at 30 °C. Cells were harvested by centrifugation (10,000 × *g*, 10 min, 4 °C) and frozen at −20 °C. Thawed cell pellets were resuspended in lysis buffer (50 mM sodium phosphate buffer, pH 8.0, 500 mM NaCl, and 10 mM imidazole) containing Complete EDTA-free protease inhibitor mixture tablets, 10 μg ml^{-1} RNase A, and 5 μg ml^{-1} DNase I, and incubated on ice for 15 min prior to disruption with an Ultrasonic Liquid Processor (Heat Systems Inc., Toronto, Ontario, Canada) fitted with a macroprobe. The resulting cell lysate was clarified by centrifugation (5,000 × *g*, 10 min, 4 °C), and the collected soluble cell fractions were mixed with Ni^{2+}-NTA agarose (2 ml $liter^{-1}$ starting culture) on a Nutator for 1 h at 4 °C. The resin slurry was poured into a disposable column and the flow-through fractions were collected. Contaminating proteins were removed from the resin by washing with 3 column volumes of lysis buffer followed by 3 column volumes of wash buffer (lysis buffer containing 20 mM imidazole). Purified $FlgJ_C$ was eluted in 5–10 ml elution buffer (lysis buffer containing 500 mM NaCl and 250 mM imidazole) and then dialyzed at 4 °C against 25 mM sodium phosphate buffer, pH 8.0.

$FlgJ_C$ was further purified by cation-exchange chromatography on Source 15S. Protein samples were applied in dialysis buffer at a flow rate of 0.7 ml min^{-1} and separation of $FlgJ_C$ from contaminants was achieved with the application of a linear gradient to 1 M NaCl. Under these conditions, $FlgJ_C$ eluted in ~80 mM NaCl.

Enzyme Activity Assays

Turbidometry—The turbidometric assay of Hash (28) was used to monitor the time course of PG solubilization by $FlgJ_C$. *Micrococcus luteus* whole cells were suspended in 25 mM citric acid, HEPES, and CHES (CCH) buffer containing 100 mM NaCl, pH 4.0, and sonicated to provide homogenous suspensions. Purified $FlgJ_C$ was added to 200-μl aliquots of substrate suspension and the decrease in turbidity of the reaction mixtures was monitored continuously at $A_{595\,nm}$ for 5 min to 1 h. For the determination of optimal pH, suspensions of PG were prepared in 25 mM CCH buffer with 100 mM NaCl, pH 3.0–8.0.

Muropeptide-based LT Assay—The HPLC-based LT assay developed by Blackburn and Clarke (29) was used to quantify the soluble muropeptides possessing 1,6-anhydromuramoyl residues released from insoluble substrate after enzyme treatment. A typical assay reaction mixture consisted of freeze-dried *S. typhimurium* PG suspended in 200 μl of 25 mM CCH buffer with 100 mM NaCl, pH 4.0, at a final concentration of 1.2 mg ml^{-1}. Reactions were initiated by the addition of enzyme followed by incubation at 37 °C with gentle shaking. Reaction mixtures lacking the addition of enzyme served as negative controls. At appropriate intervals of time, individual reactions were stopped by rapid freezing using a dry ice/ethanol bath. When required for analysis, samples were thawed and subjected to centrifugation at 13,000 × *g* for 15 min at 4 °C. To determine kinetic parameters, the soluble muropeptides recovered in the supernatants were digested with 1.1 μM mutanolysin overnight with gentle shaking at 37 °C and then reduced with 135 mM sodium borohydride for 30 min at ambient temperature. The samples were hydrolyzed to their constituent amino sugars by incubation in 6 M HCl for 1 h and 30 min at 95 °C. The hydrolyzed samples were dried *in vacuo* and resuspended in water for amino sugar analysis by HPAEC and for LC-ESI-MS analysis.

[^{18}O]H_2O-based Assay—The [^{18}O]H_2O-based peptidase assay of Lood *et al.* (30) was adapted for the assay of muropeptides that permitted differentiation between hydrolytic and LT activity, as well as facilitate direct identification of any hydrolytic reaction products associated with both soluble and insoluble fractions of PG. Freeze-dried *S. typhimurium* PG was suspended in [^{18}O]H_2O to a final concentration of 1.7 mg ml^{-1} and briefly sonicated to provide homogenous suspensions. Reactions were initiated with the addition of enzyme followed by incubation at 37 °C for 30 min with gentle shaking. Mutanolysin and *Pseudomonas aeruginosa* soluble lytic transglycosylase (Slt) 70 served as positive hydrolase (muramidase) and LT controls, respectively. Reactions were stopped by rapid freezing. They were then thawed and solubilized reaction products were separated from insoluble PG by centrifugation (15,000 × *g* for 15 min at 4 °C) prior to analysis by LC-Q-TOF-MS. The insoluble fraction was washed four to five times with 200 μl of H_2O and recovered each time by centrifugation (15,000 × *g*, 6 min, ambient temperature). The washed PG pellet was resuspended in 0.1 mM potassium phosphate buffer, pH 6.5, and solubilized by mutanolysin prior to LC-Q-TOF-MS analysis.

Identification of Reaction Products

The soluble portion of the products of a reaction of 10 mg ml^{-1} of *S. typhimurium* PG in 25 mM CCH buffer with 100 mM NaCl, pH 4.0, treated with 6.0 μM $FlgJ_C$ for 30 min at 37 °C was divided into two aliquots. One of the aliquots was further solubilized by mutanolysin and then both were reduced with $NaBH_4$ as described above. The reduced soluble reaction products were separated by RP-HPLC using a C_{18} column (ODS Hypersil 4-μm particle size, 250 × 4.6 mm, Thermo Scientific) at 45 °C previously equilibrated in 10 mM ammonium phosphate buffer, pH 5.6, containing 2% methanol at a flow rate of 0.5 ml min^{-1}. Separation was affected by application of a linear gradient to 28% methanol in the same buffer over 175 min. Eluting muropeptides were detected by monitoring $A_{210\,nm}$ and fractions collected manually were analyzed by LC-ESI-MS.

Mass Spectrometry

All MS analyses were conducted using instruments at the Mass Spectrometry Facility of the University of Guelph. LC-ESI-MS was performed using a Dionex UHPLC UltiMate 3000 liquid chromatograph interfaced to an amaZon SL ion trap mass spectrometer. Samples were injected onto a Poroshell 120 EC-C18 (2.7-μm particle size, 150 × 4.6 mm) column (Agilent) previously equilibrated at 0.2 ml/min with 0.1% formic acid in 2% acetonitrile. Separation of muropetides was achieved by application of a linear gradient to 0.1% formic acid in 100% acetonitrile over 30 min. The mass spectrometer electrospray capillary voltage was 4.5 kV and the drying temperature at 250 °C with a drying gas flow rate of 10 liters/min. Nebulizer pressure was 40 p.s.i. Nitrogen was used as both nebulizing and drying gas, and helium was used as collision gas at 60 p.s.i. The mass spectrometer scanning range was 100–2200 mass to charge in auto-MS/MS positive-ion mode.

LC-Q-TOF-MS was performed by injecting samples into an Agilent 1260 Infinity liquid chromatograph interfaced to an Agilent 6540 UHD accurate Mass Q-TOF mass spectrometer. An AdvanceBio Peptide Map C_{18} (2.1 × 100 mm) column (Agilent) was previously equilibrated at 0.2 ml min^{-1} with 0.1% formic acid containing 2% acetonitrile and separation of muropetides was achieved by application of a multistep gradient to 60% acetonitrile over 38 min and then linearly to 100% acetonitrile over 50 min. The mass spectrometer electrospray capillary voltage was maintained at 4.0 kV and the drying temperature at 350 °C with a flow rate of 5 liters min^{-1}. Nebulizer pressure was 15 p.s.i. Nitrogen was used as nebulizing and drying gas as well as collision gas. The mass-to-charge ratio was scanned across the 300–2000 range and the MS/MS mass range was scanned from 50 to 3000 m/z in positive-ion auto MS/MS mode. The auto MS/MS mode was setup to fragment 3 precursor ions per cycle (1 spectrum/s) with collision energy set 2.5 eV offset and linearly increased to 100 eV for 3000 m/z.

Other Analytical Techniques

Identification of ORFs, protein translations, and isoelectric points (pI) were performed using ApE version 2.0.47 and ProtParam (31). BlastP searches of the NCBI database for FlgJ homologs were performed using the amino acid sequence of *S. enterica* FlgJ as the probe. Analyses of sequence data were performed using ClustalW2 software (32), whereas both secondary and tertiary structure predictions were made using Phyre2 (33, 34). Nucleotide sequencing of PCR products as well as plasmids was performed by the Genomic Facility of the Advanced Analysis Center, University of Guelph. Protein concentrations were determined using the Pierce BCA protein assay kit with BSA serving as the standard (Pierce Biotechnology, Rockford, IL). SDS-PAGE on 15% acrylamide gels was conducted by the method of Laemmli (35) with Coomassie Brilliant Blue staining and Western immunoblot analysis as previously described (36). Circular dichroism (CD) spectrometry was performed as described previously (37) using a 0.1-cm path length cell at an internal temperature of 25 °C. The spectra were recorded as an average of four data accumulations, with a scan speed of 50 nm min^{-1}, bandwidth of 1 nm, 1 s, data pitch 1 nm, and range of 190–250 nm. Analyses of the spectra were performed using DichroWeb with the Selecon 3 program (38) and protein reference set 4 (39). Data were further analyzed using Contin (40).

RESULTS

In Silico Analysis of FlgJ—Multiple alignment of the amino acid sequence of *S. typhimurium* LT2 FlgJ with the known or hypothetical homologs of 61 members of the *Enterobacteriaceae* found in the genome database led to the identification of nine consensus motifs (supplemental Fig. S1). The majority of these (five) are associated with the C-terminal region of the protein, the domain that has been demonstrated to possess lytic activity (16). No structure is known for any of these enzymes, but the x-ray crystal structure of the C-terminal domain of *Sphingomonas* FlgJ ($FlgJ_C$) involving residues Gln^{154}-Asn^{310} has been determined at high resolution (20, 21).

The amino acid sequence of the putative $FlgJ_C$ of *S. typhimurium* FlgJ, involving residues Lys^{153}-His^{307}, is 43.5% identical and 72.7% similar to *Sphingomonas* sp. $FlgJ_C$ (Fig. 2). Included in this identity is Glu^{185}, the predicted catalytic residue of *Sphingomonas* $FlgJ_C$, which comprises consensus motif IV of the aligned *Enterobacteriaceae* sequences (supplemental Fig. S1). Not surprisingly given this overall similarity, the secondary structure of *S. typhimurium* $FlgJ_C$, as predicted by Phyre, is very similar to the known structure of *Sphinogomonas* $FlgJ_C$ (compare α 51.9%; β 6.4% to α 49.0%; β 9.0%, respectively) (Fig. 2). The structure of *S. typhimurium* $FlgJ_C$ predicted by Phyre using *Sphingomonas* sp. $FlgJ_C$ (Protein Data Bank (PDB) code 2ZYC) as the template (E-value, $2.3e^{-43}$; score, 253.76) consists of two lobes, α and β, separated by a deep cleft that is proposed to serve as the active site. Glu^{184} of motif IV located on the α lobe is positioned appropriately within the middle of this active site cleft to potentially serve as a catalytic acid/base.

Glu^{184} also aligns with the identified catalytic acid/base residue of *S. typhimurium* MltE. Examination of the *S. typhimurium* genome led to our identification of seven hypothetical LTs, MltA, MltB, MltC, MltD, MltE, MltF, and Slt. A phylogenic analysis of these sequences with *S. typhimurium* $FlgJ_C$ using ClustalW2 suggested that $FlgJ_C$ is most closely related to MltC or MltE (Fig. 3). Further analysis indicated that $FlgJ_C$ is more similar to MltE; MltC could not be aligned with $FlgJ_C$ using the LALIGN server, whereas $FlgJ_C$ was found to have

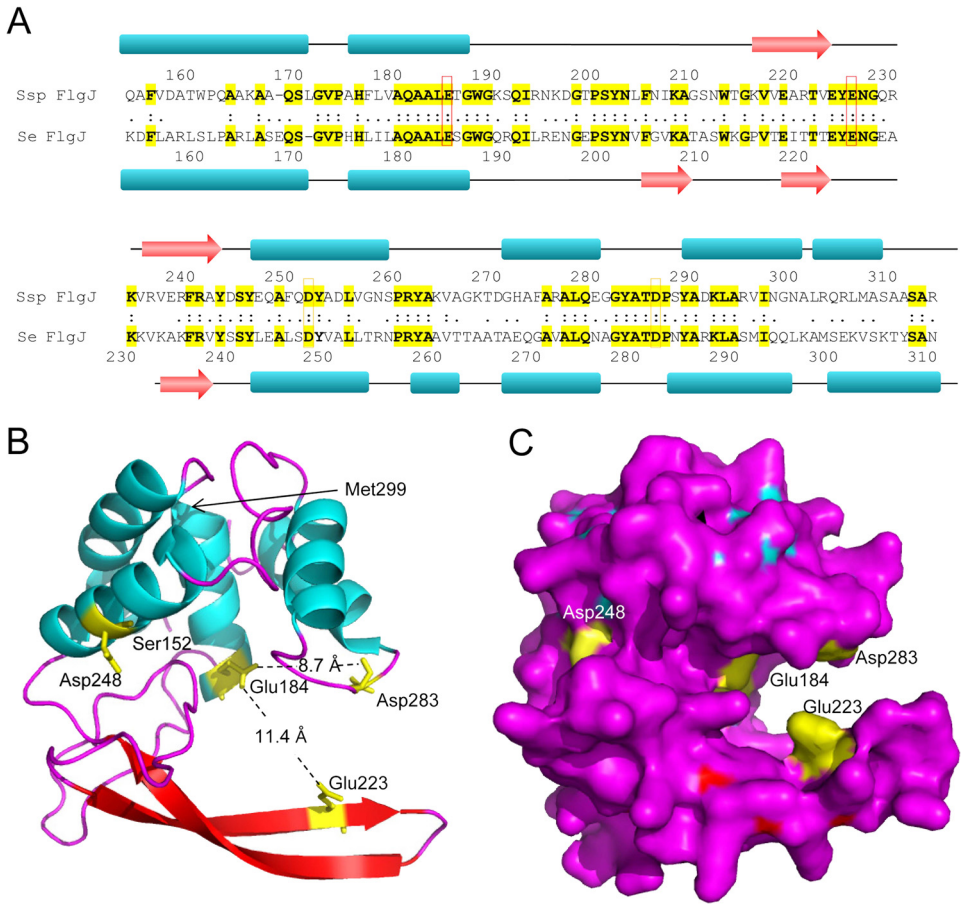

FIGURE 2. **Predicted structure of *S. enterica* $FlgJ_C$.** *A,* amino acid alignment and comparison of the known secondary structure *Sphingomonas* sp. (*Ssp*) $FlgJ_C$ with those of the *S. enterica* (*Se*) enzyme. The *red* and *orange boxes* denote the invariant Glu and Asp residues, respectively. The schematic (*B*) and surface (*C*) presentations of the predicted three-dimensional structure of *S. enterica* $FlgJ_C$. Residues 152 to 299 of the *S. enterica* $FlgJ_C$ were threaded by Phyre2 onto $FlgJ_C$ from *Sphingomonas* sp. (PDB 2ZYC). The positions of invariant Glu^{184}, Glu^{223}, Asp^{248}, and Asp^{283} are depicted in *yellow*.

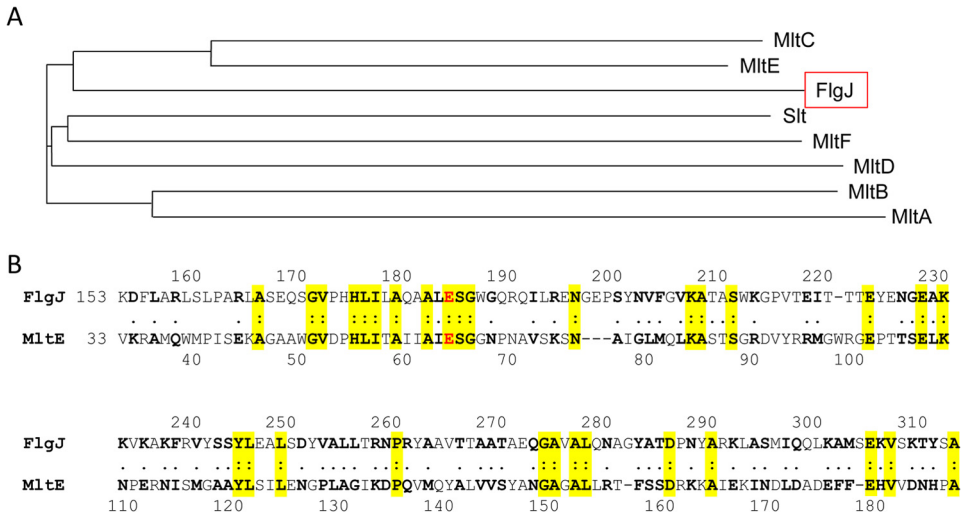

FIGURE 3. **Comparison of *S. enterica* $FlgJ_C$ primary structure with LTs.** *A,* phylogram depicting relationship of $FlgJ_C$ with the LTs identified in *S. enterica. B,* amino acid sequence alignment of $FlgJ_C$ with *S. enterica* MltE. Residues highlighted in *yellow* denote identity and the Glu residues in *red* represent the predicted catalytic acid/base residues in the respective enzymes.

10.8% identity (25% similarity) to *S. typhimurium* MltE (Fig. 3). Although this level of identity is not high, it did involve a number of residues associated with motif IV of $FlgJ_C$, including Glu^{184}. The homologous residue in MltE, Glu^{64}, comprises the signature Glu-Ser motif of the LTs and represents the sole catalytic acid/base residue. Based on these data, and that it possess the Glu-Ser LT motif, $FlgJ_C$ was proposed to function as an LT.

Overproduction and Purification of $FlgJ_C$—As observed by others previously (*e.g.* Ref. 16), attempts to prepare full-length

S. typhimurium FlgJ failed because almost all of the protein precipitated from solution during its isolation and preliminary purification. Again as found earlier, altering buffer conditions or including detergents such as Triton X-100 did not alleviate this situation. Consequently, a truncated form of FlgJ had to be engineered to provide it in soluble form for its biochemical analysis.

The *S. typhimurium flgJ* gene has been engineered previously to produce recombinant $FlgJ_C$ involving residues Ser^{152}-Phe^{316} possessing an N-terminal His_6 tag (16). We repeated this cloning by PCR amplification of the 3′ end of *flgJ* using genomic DNA of the same strain as template and ligating it into pET28a(+) giving pACFH4. Expression of this construct in *E. coli* BL21(λDE3)pLysS led to the overproduction of the protein product that was purified to apparent homogeneity (as determined by SDS-PAGE analysis; data not shown) by a combination of affinity chromatography on Ni^{2+}-NTA-agarose and cation-exchange chromatography on Source 15S. The protein remained soluble but appeared to be susceptible to degradation into a major and several minor fragments. The major fragment, which retained the N-terminal His_6 tag as observed by Western blot analysis, was found to have a molecular mass of 19.7 kDa by MALDI-TOF MS analysis (data not shown). These data indicated that cleavage was occurring at the C-terminal end of the protein to release a decapeptide. As this C-terminal decapeptide does not contain any residues of a consensus motif (supplemental Fig. S1), and hence unlikely to influence catalytic activity, a new vector (pACFH5) was generated using pACFH4 as a template, which provided a further truncation of $flgJ_C$ by 30 codons. The protein product, now lacking the 151 N-terminal and 10 C-terminal amino acid residues of FlgJ, was again purified by a combination of affinity and cation-exchange chromatographies with routine yields of 7 mg/liter of cell culture. Importantly, this form of FlgJ was found to be stable and, for convenience, it will still be referred to as $FlgJ_C$.

The secondary structure of $FlgJ_C$ was determined by CD spectroscopy involving a constrained least squares analysis. This analysis indicated the protein to be comprised of 30.8% α- and 18.6% β-structure (data not shown), which is similar to that predicted by Phyre and thus enhancing confidence in the modeled structure.

Lytic Activity of $FlgJ_C$—The turbidometric assay of Hash (28) was used to confirm the lytic activity of purified $FlgJ_C$ with *M. luteus* whole cells as substrate. As seen from the representative plot presented in Fig. 4*A*, incubation of the whole cells with $FlgJ_C$ led to the time-dependent loss of turbidity expected with the cleavage of the cell wall into soluble products by lytic enzymes. This loss of turbidity was continuous with time such that prolonged incubation led to eventual clearing of the cells, activity indicative of endo-acting lytic enzymes (15).

The dependence of this $FlgJ_C$ activity on pH was assessed by plotting initial reaction rates of turbidity loss as a function of pH using a tripartite buffer system with pH ranging from 3 to 8. Under the conditions employed, the pH-activity profile was bell shaped with a maximal lytic activity occurring at pH 4.0 (Fig. 5). The specific activity of $FlgJ_C$ at pH 4.0 was determined to be 0.33 ΔA_{600} units min^{-1} mg of $protein^{-1}$.

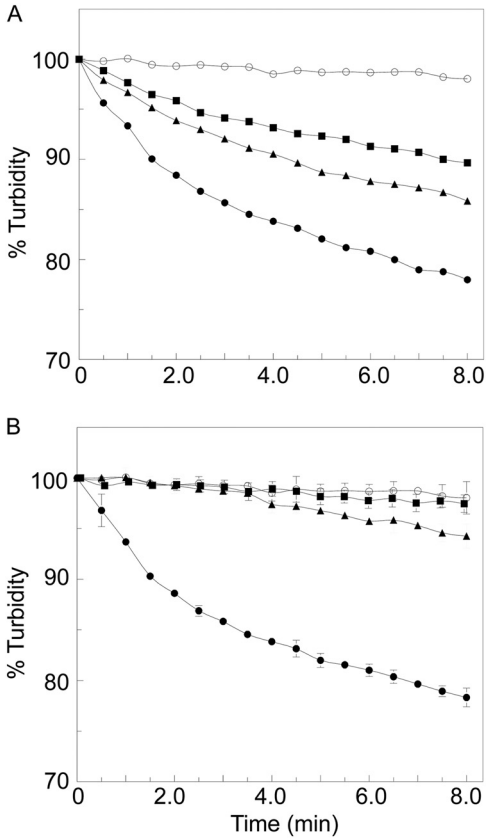

FIGURE 4. **PG lytic activity of $FlgJ_C$ and its engineered variants.** Enzyme was incubated at ambient temperature with cells of *M. luteus* suspended in 25 mM CCH buffer, pH 4.0, containing 100 mM NaCl and the progress of lysis was monitored turbidometrically at $A_{595\ nm}$. *A*, representative lytic activity of $FlgJ_C$ at varying concentrations. ○, 0 μM; ■, 1.5 μM; ▲, 3.0 μM; and ●, 6.0 μM $FlgJ_C$. *B*, activity of engineered $FlgJ_C$ variants at final concentrations of 6 μM. ○, negative control, no enzyme added; ●, wild-type $FlgJ_C$; ■, (Glu^{233} → Gln)$FlgJ_C$; and (▲) (Glu^{184} → Gln)$FlgJ_C$. The *error bars* denote S.D. ($n = 3$).

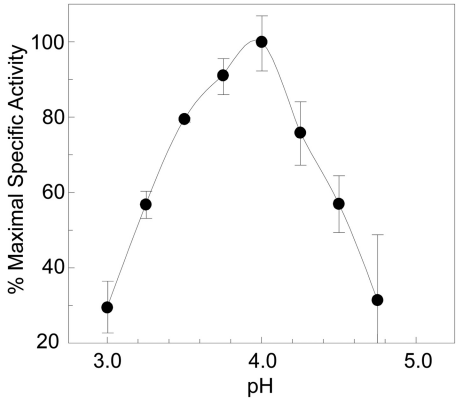

FIGURE 5. **Dependence of $FlgJ_C$ turbidometric activity on pH.** The turbidometric activity of 6.0 μM $FlgJ_C$ was determined using suspensions of purified insoluble PG as substrate in 25 mM CCH buffer with 100 mM NaCl, pH 3.0–8.0. The *error bars* denote S.D. ($n \geq 3$).

MS Analysis of $FlgJ_C$ Reaction Products—In an initial attempt to determine the reaction specificity of $FlgJ_C$, soluble reaction products from digests of *S. typhimurium* PG at pH 4.0 were recovered by centrifugation and subjected to LC-MS analysis as used previously for the analysis of muralytic reactions (*e.g.* 41). Very little soluble material was resolved by reverse-phase chromatography (Fig. 6, *trace b*) further suggesting endo-type activ-

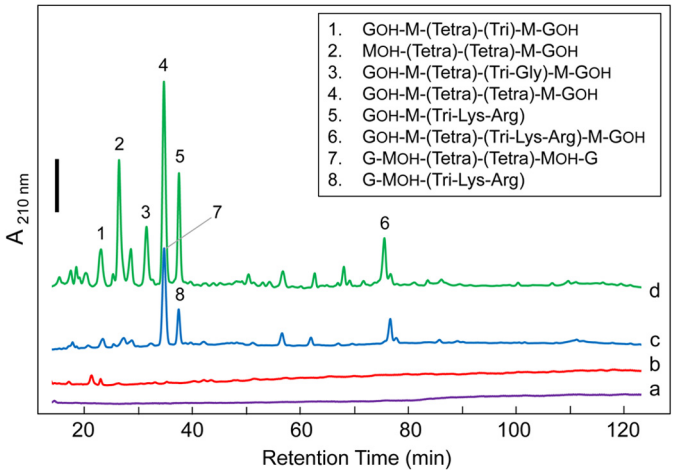

FIGURE 6. **RP-HPLC-based analysis of $FlgJ_C$ reaction products.** *S. typhimurium* PG (10 mg ml^{-1}) suspended in 25 mM CCH buffer, pH 4.0, containing 100 mM NaCl was treated with (*a*) no added enzyme; (*b*) 6.0 μM $FlgJ_C$; (*c*) 1.1 μM mutanolysin; and (*d*) 6.0 μM $FlgJ_C$ followed by 1.1 μM mutanolysin. After incubation for 30 min at 37 °C, the soluble fractions were recovered by centrifugation and then reduced with $NaBH_4$ prior to separation by RP-HPLC at 45 °C. The C_{18} column was equilibrated in 10 mM ammonium phosphate buffer, pH 5.6, containing 0.001% azide and 2% methanol at a flow rate of 0.5 ml min^{-1} and separation was affected by application of a linear gradient to 28% methanol in the same buffer over 175 min. Eluting muropeptides were detected by monitoring at $A_{210\ nm}$; the *solid black bar* denotes 0.02 absorbance units. See Table 4 for MS-based identification of muropeptides. *G*, GlcNAc; *GOH*, *N*-acetylglucosaminitol; *M*, MurNAc; *MOH*, *N*-acetylmuramitol; *Tri*, L-Ala-D-Glu-DAP; *Tetra*, L-Ala-D-Glu-DAP-D-Ala.

ity of the enzyme leading to the production of larger muropeptides that either remained associated with insoluble PG and/or were not resolved by the reverse-phase HPLC column. Subsequent treatment of the soluble products with the muramidase mutanolysin did result in the detection of a number of muropeptides (*trace d*) that were distinct from PG digests with mutanolysin alone (*trace c*). However, given the complexity of the PG substrate in terms of its heterogeneous composition (involving chains of GlcNAc-MurNAc with varying stem peptide composition and extent of cross-linking, and with each terminating in 1,6-anhydro-MurNAc residue), it was impossible to determine what the initial reaction product of $FlgJ_C$ was using this method.

$FlgJ_C$ as an LT—The HPLC-based assay developed for LTs (29) was employed to determine whether $FlgJ_C$ does indeed function as an LT. With this assay, soluble reaction products liberated from the insoluble PG substrate are reduced with $NaBH_4$, thereby converting any reducing GlcNAc and MurNAc associated with the muropeptides into their corresponding alditols, *N*-acetylglucosaminitol or *N*-acetylmuramitol, whereas any 1,6-anhydromuramic acid is left unaltered. Strong acid (6 M HCl) is then used to hydrolyze the muropeptides into their corresponding free amino sugars and amino acids, which are quantified by high pH anion-exchange chromatography-pulsed amperometric detection (HPAEC-PAD). Any 1,6-anhydromuramoyl residues generated by LT activity would be converted into muramic acid, whereas both glucosaminitol and muramitol would remain unaltered. Increasing concentrations with time of one of these products relative to the others that were intrinsic to the PG substrate defines the reaction specificity of the enzyme.

Using this method, no muramitol was detected in PG treated with $FlgJ_C$ regardless of the length of incubation indicating that

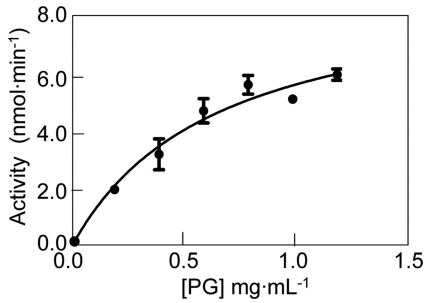

FIGURE 7. **Determination of the Michaelis-Menten parameters for $FlgJ_C$ as a *β*-*N*-acetylglucosaminidase.** *S. typhimurium* PG (0.2–1.2 mg ml^{-1}) suspended in 25 mM CCH buffer, pH 4.0, containing 100 mM NaCl was treated with 6.0 μM $FlgJ_C$ and the rates of glucosaminitol production were determined by HPAEC-based amino sugar analysis following $NaBH_4$ reduction and acid hydrolysis of muropeptide products as described under "Experimental Procedures." The *error bars* denote S.D. ($n = 3$).

$FlgJ_C$ is not a muramidase. Although muramic acid was detected in these samples (which would have originated from 1,6-anhydro-MurNAc), surprisingly its concentration did not increase significantly over time suggesting no LT activity. However, closer examination of the amino sugar analyses revealed that glucosaminitol production did increase over time. The $FlgJ_C$-catalyzed rates of glucosaminitol and muramic acid release from purified *S. typhimurium* PG as substrate at pH 4.0 were calculated to be 6.5 and 4.8 nmol min^{-1}, respectively. The faster rate of glucosaminitol production relative to that of muramic acid indicates that $FlgJ_C$ appears to function as a hydrolase and specifically as an *N*-acetylglucosaminidase.

The Michaelis-Menten parameters of $FlgJ_C$ as a *β*-*N*-acetylglucosaminidase were determined by assaying for glucosaminitol production following $NaBH_4$ reduction and acid hydrolysis of released reaction products from concentrations of PG ranging from 0.2 to 1.2 mg ml^{-1} in 25 mM CCH buffer, pH 4.0, at 37 °C (Fig. 7). Under these conditions, values of K_m and k_{cat} were determined to be 0.64 ± 0.18 mg ml^{-1} and 0.13 ± 0.016 s^{-1}, respectively.

Novel Assay for PG Hydrolytic Enzymes—A novel assay was developed to show unequivocally that $FlgJ_C$ functions as a muramidase (hydrolase). This assay involves the labeling of hydrolytic reaction products with the stable isotope of oxygen, ^{18}O, through the use of $[^{18}O]H_2O$, followed by MS analysis of reaction products. Using this heavy water, $[^{18}O]OH^-$ would be incorporated as the C-1 hydroxyl of the MurNAc or GlcNAc product following muramidase- or *β*-*N*-acetylglucosaminidase-catalyzed hydrolysis of glycosidic linkages, respectively, which would cause an increase in the abundance of the third isotope peak of the reaction products as observed by MS. As the LT-catalyzed reaction pathway does not involve H_2O, no ^{18}O could be incorporated into reaction products and hence the isotopic distribution would not be altered. To validate this assay, *S. typhimurium* PG was digested with either mutanolysin (an *N*-acetylmuramidase) or *P. aeruginosa* Slt70 in the presence of $[^{18}O]H_2O$ to serve as positive and negative controls, respectively. Soluble reaction products were collected by centrifugation and then subjected to LC-MS using a Q-TOF mass spectrometer as described under "Experimental Procedures." As expected, only the muropeptide products generated by mutanolysin contained ^{18}O. As seen in Fig. 8, the abundance of the

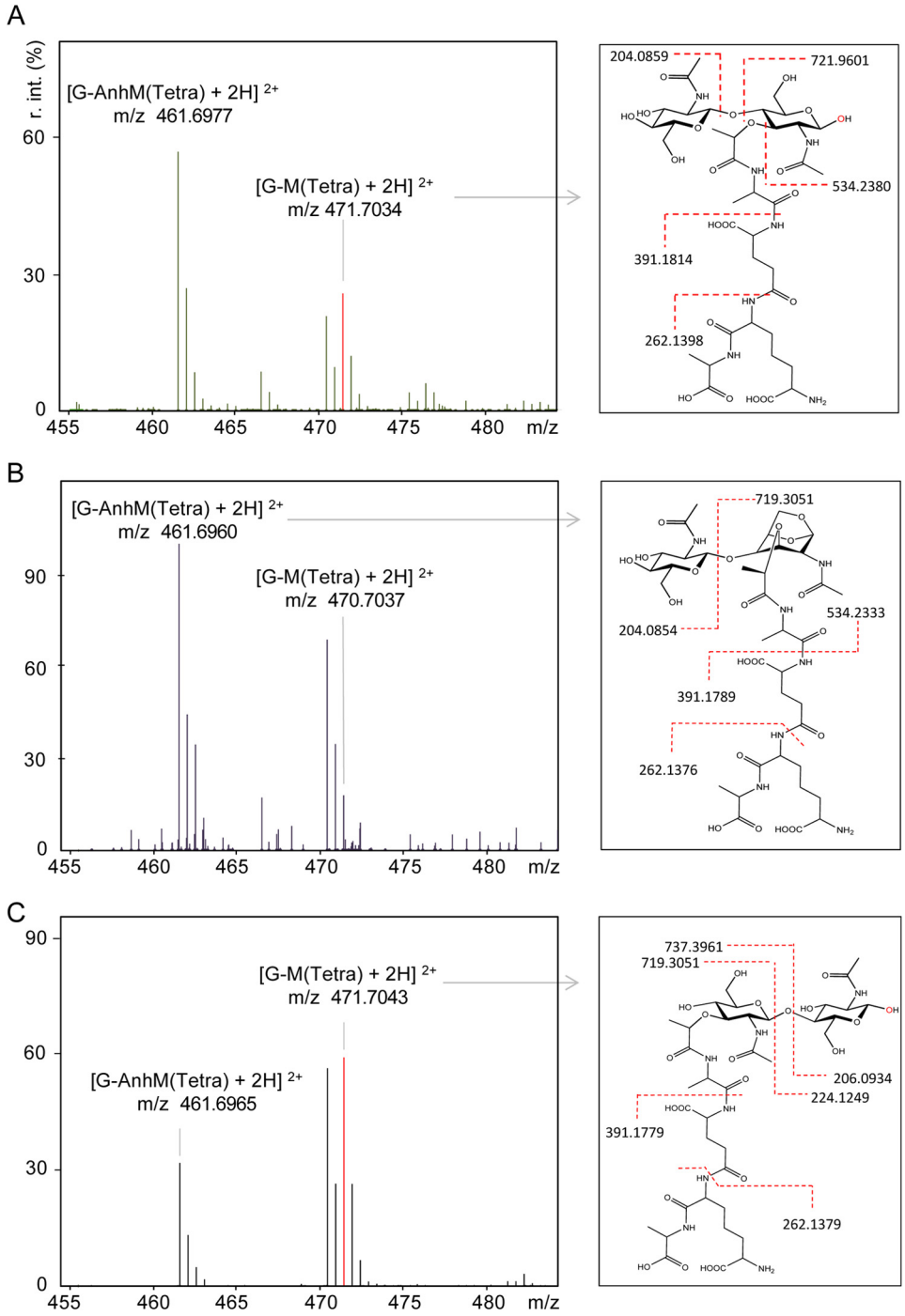

FIGURE 8. **Q-TOF MS analysis of isotopic distribution of reaction products from PG lytic enzymes.** *S. typhimurium* PG was suspended in [^{18}O]H_2O to a final concentration of 1.7 mg ml^{-1} and treated with: *A*, 1.1 μM mutanolysin; *B*, 1.0 μM *P. aeruginosa* Slt70; and *C*, 6.0 μM $FlgJ_C$. After incubation at 37 °C for 30 min, solubilized reaction products were separated from insoluble PG by centrifugation and the soluble products of each were subjected to LC-Q-TOF-MS analysis (*left panels*). For the $FlgJ_C$ reaction, the PG pellet was washed exhaustively with H_2O and then resuspended in 100 mM potassium phosphate buffer, pH 6.5, for solubilization by mutanolysin. The soluble muropeptides of this secondary digestion were recovered by centrifugation prior to LC-Q-TOF-MS analysis. The *red spectral lines* in the MS spectra denote the ^{18}O-containing isotope of the respective muropeptides. Identification of select muropeptides (as indicated) was achieved by subsequent Q-TOF MS/MS analysis (*right panels*). The monoisotopic masses $(M+H)^+$ are presented for each of the fragments detected.

third (heaviest) isotope peak of the muropetides from the mutanolysin digest were significantly increased relative to the natural abundance present in Slt70 reaction products.

Muropeptides containing high proportions of ^{18}O were detected in both the soluble and (original) insoluble reaction products after digestion of *S. typhimurium* PG in 25 mM CCH buffer, pH 4.0, prepared in [^{18}O]H_2O (Fig. 8). Tandem MS analysis of these reaction products confirmed that the muropeptides enriched with ^{18}O consisted exclusively of MurNAc-(peptides)-GlcNAc, both cross- and uncross-linked. The complete list of reaction products liberated by $FlgJ_C$ is presented in Table 3. With this knowledge, the major fractions obtained earlier by RP-HPLC (Fig. 6) that had been reduced with $NaBH_4$ were re-examined by ESI-MS and then subjected to MS/MS analysis, which

TABLE 3
Q-TOF MS/MS analysis of muropeptides released from insoluble PG by $FlgJ_C$ in the presence of $[^{18}O]H_2O$

Annotation[a]	m/z[b]			
	Expected	Observed	Δ	z
M-(tetra)-G	471.6950	471.7043	−0.0093	2
M-(tri-Lys-Arg)-G	578.2750	578.2833	−0.0083	2
[M-(tetra)-G]-[(tetra)-M-G]	621.9233	621.9323	−0.0090	3
[M-(tetra)-G]-[(tri-Lys-Arg)M-G]	692.9730	692.9859	−0.0126	3
[M-(tetra)-G]-[(tetra)M-G]-(tetra)-M-G	929.0567	929.0594	−0.0033	3

[a] G, GlcNAc; M, MurNAc; tri, L-Ala-D-Glu-DAP; tetra, L-Ala-D-Glu-DAP-D-Ala.
[b] The m/z data presented correspond to the ^{18}O isotope-containing muropeptides.

revealed muropeptides possessing glucosaminitol (Table 4). These data thus confirm that $FlgJ_C$ functions as a hydrolase, and specifically as a β-*N*-acetylglucosaminidase.

Identification of Catalytic Residues $FlgJ_C$—Typically, the mechanism of action of glycoside hydrolases involves two acidic amino acid residues that are opposed to each other across the active site cleft/pocket. Glu^{223} had been identified earlier as an essential residue in $FlgJ_C$ from both *S. typhimurium* (16) and *Sphingomonas* sp. (20, 21), and this invariant residue comprises motif VI of the aligned sequences of identified *Enterobacteriaceae* FlgJs (supplemental Fig. S1). However, these earlier studies report different potential second catalytic residues. Asp^{248} was proposed to serve this function in *S. typhimurium* $FlgJ_C$ although its replacement did not greatly reduce catalytic activity; only a semiquantitative zymogram assay was used to assess enzyme activity (16). Although this residue is also invariant among the FlgJs of the *Enterobacteriaceae,* comprising motif VII, it would appear to be positioned to the side of the active site cleft and too far from any other acidic residues (Fig. 2, *B* and *C*). With the understanding of the crystal structure of the *Sphingomonas* sp. $FlgJ_C$, Glu^{185} was identified to function as the catalytic acid/base residue (20, 21). The homologous Glu^{184} of *S. typhimurium* $FlgJ_C$ is positioned directly opposite Glu^{223} on the other side of the putative active site cleft in the predicted structure of the enzyme at a distance of 11.4 Å away (Fig. 2, *B* and *C*).

To confirm their participation in the catalytic mechanism of *S. typhimurium* $FlgJ_C$, both Glu^{184} and Glu^{223} were replaced with glutamine by site-directed mutagenesis using pACFH5 as the template. These two forms of $FlgJ_C$ were purified to apparent homogeneity using the same protocol used for the wild-type form of the enyzme (data not shown) and CD spectroscopy was used to confirm that their secondary structures were not altered with the amino acid replacement. The resulting spectra were found to be indistinguishable from that of the wild-type enzyme (data not shown).

The specific activity of each of the FlgJ forms was determined using the turbidometric assay with 0.4 mg ml^{-1} *M. luteus* whole cells as substrate at pH 4 (Fig. 4*B*). The activity of $(Glu^{223} \rightarrow Gln)FlgJ_C$ was barely detectable and its calculated specific activity was 0.14% of that of the wild-type enzyme (Table 5). $(Glu^{184} \rightarrow Gln)FlgJ_C$ was also weakly active but it did retain 8.8% wild-type activity under the conditions employed.

DISCUSSION

This study presents the first biochemical analysis of the enzymatic activity of FlgJ, an important protein involved in the flagellar biosynthetic pathway of many Gram-negative bacterial pathogens. Contrary to what has been proposed/discussed in the past, the enzyme is neither a muramidase nor an LT but rather it functions as an endo-acting β-*N*-acetylglucosaminidase. Moreover, two acidic residues appear to be essential for this catalytic activity.

Despite being identified 15 years ago (16), the nature of the lytic activity of FlgJ had not been determined, likely because of the significant technical limitations associated with studying PG-degrading enzymes. The heterogeneity of both the substrate and resulting lytic products in terms of stem peptide composition and extent of cross-linking, as well as any modification to the glycan chains, contribute to the complexity in the analysis of the PG-related material. With the lack of a soluble, defined and commercially available substrate, researchers based their assessment and interpretations on zymogram and/or turbidometric assays coupled with amino acid sequence alignments and structural homologies.

Our initial attempts at identifying reaction products released from $FlgJ_C$ involved RP-HPLC coupled with ESI-MS/MS. This has been used successfully in the past to characterize the activity of exo-acting lytic enzymes that release a limited number of soluble dissacharide-based muropeptides, which proved to be relatively easy to identify (*e.g.* Ref. 42). However, a low abundance of these products was observed in the soluble fraction of $FlgJ_C$ reactions suggesting endo-type activity where glycan reaction products would remain attached, either directly or through cross-linking, to the PG sacculi substrate. To overcome this limitation, we developed a novel assay that permitted the direct labeling of hydrolytic reaction products with the stable ^{18}O isotope of $[^{18}O]H_2O$ coupled with MS and compositional analyses. A major advantage of this assay is that it allows for (i) precise determination of reaction products generated by hydrolytic enzymes in both the soluble and insoluble fractions where the latter require subsequent enzymatic or acid digestion prior to analysis, and (ii) simultaneous discrimination between hydrolytic and non-hydrolytic reactions.

In the present study, the observed increase in production of glucosaminitol over time (after $NaBH_4$ reduction of reaction products) coupled with the introduction of ^{18}O into only GlcNAc residues facilitated the identification of FlgJ as being hydrolytic and, specifically, a β-*N*-acetylglucosaminidase. Furthermore, that the majority of the labeled GlcNAc was found in the insoluble fraction of reactions indicated FlgJ is endo-acting. This latter finding was not unexpected given the function of FlgJ to create pores within the existing PG sacculus for flagella assembly. *S. typhimurium* possesses 6–8 peritrichous flagella (43) as well as the ability to become hyperflagellated during periods of stress (44). Thus, flagellar assembly would require

TABLE 4
Electrospray ionization-MS analysis of muropeptides released from insoluble PG by $FlgJ_C$

Fraction No.[a]	Annotation[b]	*m/z*			
		Expected	Observed	Δ	*z*
1	GOH-M-(tetra)-(tri)-M-GOH	897.8850	897.8993	−0.0143	2
2	MOH-(tetra)-(tetra))-M-GOH	831.8450	831.8759	−0.0309	2
3	GOH-M-(tetra)-(tri-Gly)-M-GOH	617.9233	617.9461	−0.0228	3
4	GOH-M-(tetra)-(tetra)-M-GOH	933.4000	933.4129	−0.0129	2
5	GOH-M- (tri-Lys-Arg)	578.2850	578.2947	−0.0097	2
6	GOH-M-(tetra)-(tri-Lys-Arg)-M-GOH	1039.9800	1039.9914	−0.0114	2
7	G-MOH-(tetra)-(tetra)-MOH-G	933.4000	933.4171	−0.0171	2
8	G-MOH- (tri-Lys-Arg)	578.2850	578.2905	−0.0055	2

[a] The muropeptide fractions correspond to those of the RP-HPLC separation presented in Fig. 6.
[b] Identification of each muropeptide was made by MS/MS analysis of each parent ion (data not shown). G, GlcNAc; GOH, *N*-acetylglucosaminitol; M, MurNAc; MOH, *N*-acetylmuramitol; tri, L-Ala-D-Glu-DAP; tetra, L-Ala-D-Glu-DAP-D-Ala.

TABLE 5
Specific activities of $FlgJ_C$ and its engineered variants

Enzyme	Specific activity	
	$\Delta OD_{595}\ min^{-1} mg\ protein^{-1}$	%
Wild-type $FlgJ_C$	3.29×10^{-1}	100
($Glu^{184} \rightarrow Gln$)	2.90×10^{-2}	8.82
($Glu^{223} \rightarrow Gln$)	4.51×10^{-4}	0.14

the activity of an endo-acting lytic to create these pores along the PG sacculus at varying positions distinct from regions of continuing growth or division where other autolysins (*e.g.* LTs) function (11–13, 15).

This study introduces the first characterized β-*N*-acetylglucosaminidase found in Gram-negative bacteria. Based on structural (primary, secondary, and tertiary) information, $FlgJ_C$ from *Sphingomonas* sp. strain A1 had been classified as a member of the glycoside hydrolase family GH73 (20) of the CAZy database. This family is comprised largely of β-*N*-acetylglucosaminidases from Gram-positive bacteria. Hence, perhaps it should have been predicted earlier, if not expected, that FlgJ functions as a β-*N*-acetylglucosaminidase. Presumably, the lack of prior identification of this activity in Gram-negative bacteria together with knowledge of its structure possessing a lysozyme-fold led to is incorrect assignment by some as a muramidase. Identification of enzyme specificity became complicated with observations that FlgJ shares sequence identity with family 1E LTs, enzymes that also possess the lysozyme-fold and represent the major class of autolysin with glycolytic activity in Gram-negative bacteria (15, 41). Given this, the misassignment of FlgJ as an LT is understandable.

Another commonality shared between many β-*N*-acetylglucosaminidases and LTs is their putative substrate-assisted mechanisms of action. Typical glycolytic enzymes catalyze either single- or double-displacement reactions involving the direct participation of two catalytic residues (usually Glu and/or Asp), which are appropriately spaced across the active site. However, the family of GH18, GH20, GH84, and likely, GH85 β-*N*-acetylglucosaminidases have been shown to invoke the anchimeric assistance of the *N*-acetyl group of their GlcNAc-based substrate in their mechanism of action (45–47). In this mechanism, the carbonyl oxygen of the acetyl group of substrate substitutes for a nucleophilic catalytic residue to generate an oxazolinium ion intermediate that stabilizes the oxocarbenium ion transition state formed by acid catalysis during glycolytic cleavage (Fig. 9). Assistance in rendering the carbonyl oxygen nucleophilic is provided by a second acidic amino acid residue positioned appropriately to deprotonate the *N*-acetamido nitrogen, but distant from the catalytic acid/base residue. A similar mechanism of action has been proposed for the LTs of families GH23, GH102, GH103, and GH104 (Ref. 48, and references therein). With the GH73 enzymes, the situation is much less clear.

The structures of three GH73 enzymes are now known, those of *L. monocytogenes* Auto (PDB 3F17), *S. pneumoniae* LytB (PDB 4Q2W), and FlgJ from *Sphingomonas* sp. (PDB 2ZYC). All share an α/β-hydrolase-fold with a deep cleft that accommodates their glycan substrates and a conserved active site. With each, the identities of the catalytic acid/base residues is clear and they (21, 49, 50), together with the homolog of *Staphylococcus warneri* Atl (51), have been proven experimentally. These findings were confirmed in the current study with the significant decrease in catalytic activity found with *S. typhimurium* ($Glu^{184} \rightarrow Gln$)$FlgJ_C$. The residual activity observed may reflect the relatively low pH at which the enzyme assay was performed that may have facilitated acid catalysis.

The identification of a catalytic nucleophile/base residue, however, has been inconclusive with varying results obtained from different mutational studies. These studies have supported either a single displacement, inverting mechanism of action (21, 52) or one involving substrate assistance (49, 51). Our replacement of *S. typhimurium* $FlgJ_C$ Glu^{223} with Gln led to an almost complete loss of activity (0.14% residual) strongly suggesting the direct participation of this residue as the base catalyst in an inverting mechanism of action. However, the residue is predicted to be positioned 11.4 Å from the catalytic acid Glu^{184} (Fig. 2), which represents an outer limit for the distance between catalytic residues in an inverting enzyme (53) (Fig. 9). Interestingly, Glu^{223} is located on a flexible loop that forms the active site cleft and this loop has been proposed to undergo a conformational change upon binding substrate (21), an implication that has been made for other GH73 *N*-acetylglucosaminidases such as Auto (52). Thus, it remains to be established whether this loop does indeed close to permit an inverting mechanistic pathway, or instead positions Glu^{233} allowing it to assist the deprotonation of the amide of an *N*-acetyl group in an anchimeric mode of action resulting in the retention of anomeric configuration in the lytic product.

Knowledge of the stereochemistry of the initial reaction products would help to identify whether the enzyme catalyzes an inverting or a retaining mechanism. Typically, this is assessed by conducting substrate hydrolyzes in an NMR for the

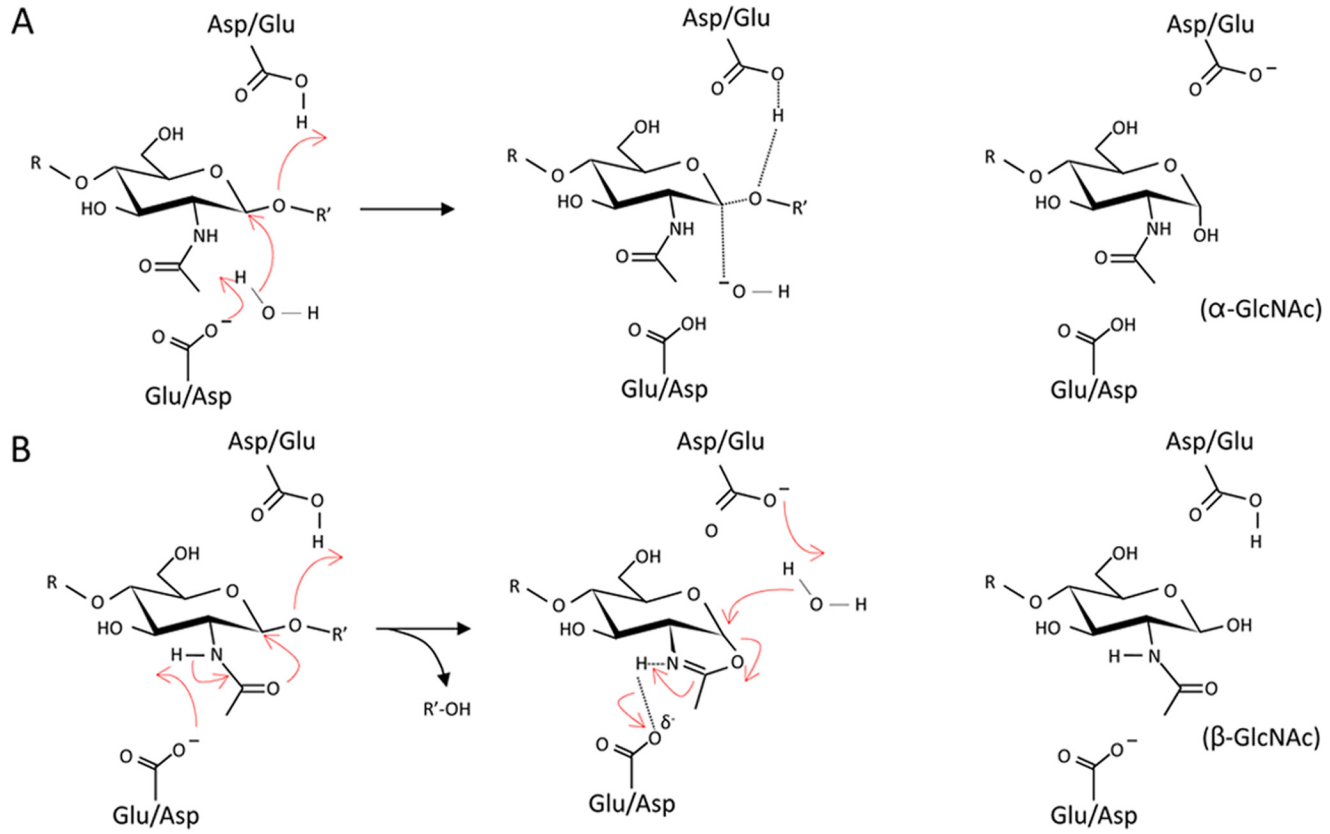

FIGURE 9. **Proposed mechanisms of inverting and retaining *β*-*N*-acetylglucosaminidases.** *A,* with the single-displacement mechanism, a catalytic acid protonates the oxygen of the *β*-1,4 glycosidic linkage facilitating the departure of the first product, whereas a catalytic base abstracts a proton from water allowing it to directly attack the anomeric C-1 carbon of the GlcNAc residue with inversion of configuration to the α-GlcNAc product. *B,* in the anchimeric double-displacement mechanism, acid catalysis proceeds as described above, whereas the carbonyl oxygen of the substrate acetamido group acts as a nucleophile, with assistance from the catalytic base residue through deprotonation of the amide N, leading to the formation of the oxazolinium ion intermediate. The catalytic acid then acts as a base to abstract a proton from the nucleophilic water, which attacks the C-1 of the GlcNAc residue to hydrolyze the oxazolinium ion leading to retention of anomeric configuration.

immediate analysis of initial products but this experiment would prove technically challenging, if not impossible, for FlgJ given its endo activity on the totally insoluble PG substrate. However, this investigation could also be assisted by inhibition studies with GlcNAc-thiazoline, a mechanism-based inhibitor of *N*-acetylglucosaminidases that use substrate-assisted catalysis (CAZy database) (24).

In a recent study, Roure *et al.* (22) demonstated that endogenous LTs are required for full motility of both *Helicobacter pylori* and *S. typhimurium*. However, these lytic enzymes were not required for insertion or assembly of the flagella complex within cells walls (mutants deficient in the genes encoding the specific LTs still possessed flagella) but rather for the proper functioning of the flagellar motor protein MotB. The LTs were postulated to provide 1,6-anhydromuramoyl residues through which MotB could bind covalently to secure the motor complex within the PG sacculus. It was assumed that pores within the PG network of the sacculus would be large enough to accommodate the flagellum complex without any specific remodeling. Our observations, together with earlier findings on the requirement of FlgJ, suggest that the *N*-acetylglucosaminidase activity associated with this protein is required to generate the appropriate pores for flagella insertion that are then modified by an LT to provide binding sites for the motor complex. Why two distinct lytic enzymes would be required for this purpose rather than the use of an LT alone to create both the pore and appropriate binding sites for the flagellum remains unknown. It is also curious that these Gram-negative cells utilize an *N*-acetylglucosaminidase for this lysis and not a muramidase. It is possible that the *N*-acetylglucosaminidase domain of FlgJ represents an evolutionary link to flagellated Gram-positive bacteria given that *N*-acetylglucosaminidases represent their major autolysins (13) and they are indeed required for flagella insertion in these bacteria (Ref. 22 and references therein). Regardless, the low pH activity optimum of $FlgJ_C$ of 4.0 is consistent with its autolytic role that would require the localization of the enzyme to the periplasm at the cytoplasmic membrane-PG interface. It would be expected that the pH of this microenvironment would be low due to the maintenance of a protonmotive force, the source of energy that will be used by the flagellar motor for motility.

Motility of pathogenic bacteria is a major virulence factor as it allows them to reach and colonize their specific environmental niches. Thus, targeting the assembly of motility appendages essential for bacterial survival may aid in the fight against bacterial infections and diseases. Knowledge of the specific type of lytic activity associated with flagella assembly is essential if the enyzmes responsible are to be targeted for inhibitor development. Moreover, our development of a novel assay based on the incorporation of ^{18}O into hydrolytic products will greatly facil-

itate the characterization of other PG lytic enzymes that continue to be discovered as the metabolism of this important bacterial cell wall polymer is further explored.

Acknowledgments—We thank Dyanne Brewer and Armen Charchoglyan of the Mass Spectrometry Facility (Advanced Analysis Centre, University of Guelph) and Josh Kaplansky for expert technical assistance and both Dave Sychantha and Chris Vandenende for helpful discussions.

REFERENCES

1. Moens, S., and Vanderleyden, J. (1996) Functions of bacterial flagella. *Crit. Rev. Microbiol.* **22,** 67–100
2. Berger, C. N., Shaw, R. K., Brown, D. J., Mather, H., Clare, S., Dougan, G., Pallen, M. J., and Frankel, G. (2009) Interaction of *Salmonella enterica* with basil and other salad leaves. *ISME J.* **3,** 261–265
3. Eaves-pyles, T., Murthy, K., Liaudet, L., Virág, L., Ross, G., Soriano, F. G., and Salzman, A. L. (2001) Flagellin, a novel mediator of *Salmonella*-induced epithelial activation and systemic inflammation: IκBα degradation, induction of nitric oxide synthase, induction of proinflammatory mediators, and cardiovascular dysfunction. *J. Immunol.* **166,** 1248–1260
4. Apel, D., and Surette, M. G. (2008) Bringing order to a complex molecular machine: the assembly of the bacterial flagella. *Biochim. Biophys. Acta* **1778,** 1851–1858
5. Young, G. M., Schmiel, D. H., and Miller, V. L. (1999) A new pathway for the secretion of virulence factors by bacteria: the flagellar export apparatus functions as a protein-secretion system. *Proc. Natl. Acad. Sci. U.S.A.* **96,** 6456–6461
6. Nambu, T., Inagaki, Y., and Kutsukake, K. (2006) Plasticity of the domain structure in FlgJ, a bacterial protein involved in flagellar rod formation. *Genes Genet. Syst.* **81,** 381–389
7. Kubori, T., Shimamoto, N., Yamaguchi, S., Namba, K., and Aizawa, S. (1992) Morphological pathway of flagellar assembly in *Salmonella typhimurium*. *J. Mol. Biol.* **226,** 433–446
8. Suzuki, T., Iino, T., Horiguchi, T., and Yamaguchi, S. (1978) Incomplete flagellar structures in non-flagellate mutants of *Salmonella typhimurium*. *J. Bacteriol.* **133,** 904–915
9. Suzuki, H., Yonekura, K., Murata, K., Hirai, T., Oosawa, K., and Namba, K. (1998) A structural feature in the central channel of the bacterial flagellar FliF ring complex is implicated in type III protein export. *J. Struct. Biol.* **124,** 104–114
10. Demchick, P., and Koch, A. L. (1996) The permeability of the wall fabric of *Escherichia coli* and *Bacillus subtilis*. *J. Bacteriol.* **178,** 768–773
11. Vollmer, W., and Bertsche, U. (2008) Murein (peptidoglycan) structure, architecture and biosynthesis in *Escherichia coli*. *Biochim. Biophys. Acta* **1778,** 1714–1734
12. van Heijenoort, J. (2011) Peptidoglycan hydrolases of *Escherichia coli*. *Microbiol. Mol. Biol. Rev.* **75,** 636–663
13. Vollmer, W., Joris, B., Charlier, P., and Foster, S. (2008) Bacterial peptidoglycan (murein) hydrolases. *FEMS Microbiol. Rev.* **32,** 259–286
14. Höltje, J.-V., Mirelman, D., Sharon, N., and Schwarz, U. (1975) Novel type of murein transglycosylase in *Escherichia coli*. *J. Bacteriol.* **124,** 1067–1076
15. Scheurwater, E., Reid, C. W., and Clarke, A. J. (2008) Lytic transglycosylases: bacterial space-making autolysins. *Int. J. Biochem. Cell Biol.* **40,** 586–591
16. Nambu, T., Minamino, T., Macnab, R. M., and Kutsukake, K. (1999) Peptidoglycan-hydrolyzing activity of the FlgJ protein, essential for flagellar rod formation in *Salmonella typhimurium*. *J. Bacteriol.* **181,** 1555–1561
17. Dijkstra, A. J., and Keck, W. (1996) Peptidoglycan as a barrier to transenvelope transport. *J. Bacteriol.* **178,** 5555–5562
18. Das, M., Chopra, A. K., Wood, T., and Peterson, J. W. (1998) Cloning, sequencing and expression of the flagellin core protein and other genes encoding structural proteins of the *Vibrio cholerae* flagellum. *FEMS Microbiol. Lett.* **165,** 239–246
19. Hirano, T., Minamino, T., and Macnab, R. M. (2001) The role in flagellar rod assembly of the N-terminal domain of *Salmonella* FlgJ, a flagellum-specific muramidase. *J. Mol. Biol.* **312,** 359–369
20. Hashimoto, W., Ochiai, A., Momma, K., Itoh, T., Mikami, B., Maruyama, Y., and Murata, K. (2009) Crystal structure of the glycosidase family 73 peptidoglycan hydrolase FlgJ. *Biochem. Biophys. Res. Commun.* **381,** 16–21
21. Maruyama, Y., Ochiai, A., Itoh, T., Mikami, B., Hashimoto, W., and Murata, K. (2010) Mutational studies of the peptidoglycan hydrolase FlgJ of *Sphingomonas* sp. strain A1. *J. Basic Microbiol.* **50,** 311–317
22. Roure, S., Bonis, M., Chaput, C., Ecobichon, C., Mattox, A., Barrière, C., Geldmacher, N., Guadagnini, S., Schmitt, C., Prévost, M. C., Labigne, A., Backert, S., Ferrero, R. L., and Boneca, I. G. (2012) Peptidoglycan maturation enzymes affect flagellar functionality in bacteria. *Mol. Microbiol.* **86,** 845–856
23. de la Mora, J., Ballado, T., González-Pedrajo, B., Camarena, L., and Dreyfus, G. (2007) The flagellar muramidase from the photosynthetic bacterium *Rhodobacter sphaeroides*. *J. Bacteriol.* **189,** 7998–8004
24. Mark, B. L., Vocadlo, D. J., Knapp, S., Triggs-Raine, B. L., Withers, S. G., and James, M. N. (2001) Crystallographic evidence for substrate-assisted catalysis in a bacterial beta-hexosaminidase. *J. Biol. Chem.* **276,** 10330–10337
25. de la Mora, J., Osorio-Valeriano, M., González-Pedrajo, B., Ballado, T., Camarena, L., and Dreyfus, G. (2012) The C terminus of the flagellar muramidase SltF modulates the interaction with FlgJ in *Rhodobacter sphaeroides*. *J. Bacteriol.* **194,** 4513–4520
26. Viollier, P. H., and Shapiro, L. (2003) A lytic transglycosylase homologue, PleA, is required for the assembly of pili and the flagellum at the *Caulobacter crescentus* cell pole. *Mol. Microbiol.* **49,** 331–345
27. Clarke A. J. (1993) Compositional analysis of peptidoglycan by high performance anion-exchange chromatography. *Anal. Biochem.* **212,** 344–350
28. Hash, J. H. (1967) Measurement of bacteriolytic enzymes. *J. Bacteriol.* **93,** 1201–1202
29. Blackburn, N. T., and Clarke, A. J. (2000) Assay for lytic transglycosylases: a family of peptidoglycan lyases. *Anal. Biochem.* **284,** 388–393
30. Lood, R., Raz, A., Molina, H., Euler, C. W., and Fischetti, V. A. (2014) A highly active and negatively charged *Streptococcus pyogenes* lysine with a rare D-alanyl-L-alanine endopeptidase activity protects mice against streptococcal bacteremia. *Antimicrob. Agents Chemother.* **58,** 3073–3084
31. Gasteiger E., Hoogland C., Gattiker A., Duvaud S., Wilkins M. R., Appel R. D., Bairoch A. (2005) in *The Proteomics Protocols Handbook* (Walker, J. M., ed) pp. 571–607, Humana Press, Totowa, NJ
32. Chenna, R., Sugawara, H., Koike, T., Lopez, R., Gibson, T. J., Higgins, D. G., and Thompson, J. D. (2003) Multiple sequence alignment with the Clustal series of programs. *Nucleic Acids Res.* **31,** 3497–3500
33. Bennett-Lovsey, R. M., Herbert, A. D., Sternberg, M. J., and Kelley, L. A. (2008) Exploring the extremes of sequence/structure space with ensemble fold recognition in the program Phyre. *Proteins* **70,** 611–625
34. Kelley, L. A., MacCallum, R. M., and Sternberg, M. J. (2000) Enhanced genome annotation using structural profiles in the program 3D-PSSM. *J. Mol. Biol.* **299,** 499–520
35. Laemmli, U. K. (1970) Cleavage of structural proteins during the assembly of the head of bacteriophage T4. *Nature* **227,** 680–685
36. Moynihan, P. J., and Clarke, A. J. (2010) *O*-Acetylation of peptidoglycan in Gram-negative bacteria: identification and characterization of peptidoglycan *O*-acetyltransferase in *Neisseria gonorrhoeae*. *J. Biol. Chem.* **285,** 13264–13273
37. Pfeffer, J. M., Weadge, J. T., and Clarke, A. J. (2013) Mechanism of action of *Neisseria gonorrhoeae O*-acetylpeptidoglycan esterase, an SGNH serine esterase. *J. Biol. Chem.* **288,** 2605–2613
38. Sreerama, N., Venyaminov, S. Y., and Woody, R. W. (1999) Estimation of the number of helical and strand segments in proteins using CD spectroscopy. *Protein Sci.* **8,** 370–380
39. Sreerama, N., Venyaminov, S. Y., and Woody, R. W. (2000) Estimation of protein secondary structure from CD spectra: Inclusion of denatured proteins with native protein in the analysis. *Anal. Biochem.* **287,** 243–251
40. van Stokkum, I. H., Spoelder, H. J., Bloemendal, M., van Grondelle, R., and Groen, F. C. (1990) Estimation of protein secondary structure and error

analysis from CD spectra. *Anal. Biochem.* **191,** 110–118
41. Blackburn, N. T., and Clarke, A. J. (2001) Identification of four families of peptidoglycan lytic transglycosylases. *J. Mol. Evol.* **52,** 78–84
42. Blackburn, N. T., and Clarke, A. J. (2002) Characterization of soluble and membrane-bound family 3 lytic transglycosylases from *Pseudomonas aeruginosa*. *Biochemistry* **41,** 1001–1013
43. Fujii, M., Shibata, S., and Aizawa, S-I. (2008) Polar, peritrichous, and lateral flagella belong to three distinguishable flagellar families. *J. Mol. Biol.* **379,** 273–283
44. Harshey, R. M., and Matsuyama, T. (1994) Dimorphic transistion in *Escherichia coli* and *Salmonella typhimurium*: surface-induced differentiation into hyperflagellate swarmer cells. *Proc. Natl. Acad. Sci. U.S.A.* **91,** 8631–8635
45. Terwisscha van Scheltinga, A. C., Armand, S., Kalk, K. H., Isogai, A., Henrissat, B., and Dijkstra, B. W. (1995) Stereochemistry of chitin hydrolysis by a plant chitinase/lysozyme and x-ray structure of a complex with allosamidin: evidence for substrate assisted catalysis. *Biochemistry* **34,** 15619–15623
46. Tews, I., Perrakis, A., Oppenheim, A., Dauter, Z., Wilson, K. S., and Vorgias, C. E. (1996) Bacterial chitobiase structure provides insight into catalytic mechanism and the basis of Tay-Sachs disease. *Nat. Struct. Biol.* **3,** 638–648
47. Drouillard, S., Armand, S., Davies, G. J., Vorgias, C. E., and Henrissat, B. (1997) *Serratia marcescens* chitobiase is a retaining glycosidase utilizing substrate acetamido group participation. *Biochem. J.* **328,** 945–949
48. Reid, C. W., Blackburn, N. T., Legaree, B. A., Auzanneau, F.-I., and Clarke, A. J. (2004) Inhibition of membrane-bound lytic transglysosylase by NAG-thiazoline. *FEBS Lett.* **574,** 73–79
49. Inagaki, N., Iguchi, A., Yokoyama, T., Yokoi, K. J., Ono, Y., Yamakawa, A., Taketo, A., and Kodaira, K. (2009) Molecular properties of the glucosaminidase AcmA from *Lactococcus lactis* MG1363: mutational and biochemical analyses. *Gene* **447,** 61–71
50. Bai, X.-H., Chen, H.-J., Jiang, Y. L., Wen, Z., Huang, Y., Cheng, W., Li, Q., Lei, Q., Zhang, J.-R., Chen, Y., and Zhou, C. Z. (2014) Structure of pneumococcal peptidoglycan hydrolase LytB reveals insights into the bacterial cell wall remodeling and pathogenesis. *J. Biol. Chem.* **289,** 23403–23416
51. Yokoi, K. J., Sugahara, K., Iguchi, A., Nishitani, G., Ikeda, M., Shimada, T., Inagaki, N., Yamakawa, A., Taketo, A., and Kodaira, K. (2008) Molecular properties of the putative autolysin Atl(WM) encoded by *Staphylococcus warneri* M: mutational and biochemical analyses of the amidase and glucosaminidase domains. *Gene* **416,** 66–76
52. Bublitz, M., Polle, L., Holland, C., Heinz, D. W., Nimtz, M., and Schubert, W. D. (2009) Structural basis for autoinhibition and activation of Auto, a virulence-associated peptidoglycan hydrolase of *Listeria monocytogenes*. *Mol. Microbiol.* **71,** 1509–1522
53. McCarter, J. D., and Withers, S. G. (1994) Mechanisms of enzymatic glycoside hydrolysis. *Curr. Opin. Struct. Biol.* **4,** 885–892